

Hybrid Bohm and classical diffusion in a strongly magnetized plasma

Y. Furutani and Y. Oda

*Department of Electronics, School of Engineering, Okayama University,
Tsushimanaka 3-1-1, Okayama 700, Japan*

C. Deutsch and M. M. Gombert

Laboratoire de Physique des Gaz et des Plasmas, Université de Paris-Sud,
Centre d'Orsay, 91400 Orsay, France*

(Received 26 March 1982)

Accurate static structure factors, which take into account short-ranged (diffraction and symmetry) quantum effects in a strongly magnetized electron-ion plasma, are introduced in a guiding-center formulation. Quantum and classical analytic expressions are, respectively, obtained for the hydrodynamic (Bohm) ($\beta_{cl} + \beta_{qu} \sim 1/B$) and the kinetic ($\alpha_{cl} + \alpha_{qu} \sim 1/B^2$) contributions to the complete hybrid diffusion. (B denotes the magnetic fields strength.) In a certain range of (B, T) parameters, one obtains $\beta_{qu} \sim \alpha_{cl}$. Large B values are shown to extend the validity of a classical calculation.

I. INTRODUCTION

We are currently reviving the problem of the particle transport in a strongly magnetized and fully ionized plasma. The experimental demands arise mostly from three distinct and very important areas: electron-positron plasmas in the pulsar magnetosphere,¹ electron-hole plasmas in strongly magnetized and heavily doped semiconductors,² and transport in the vicinity of hot spots in laser-produced plasmas.³

The density and temperature domains thus considered are enormous: n_e ranges from 10^{10} to 10^{21} cm^{-3} , while T_e , the electron temperature, is located between 10^2 and 10^7 K. Nevertheless, these systems share in common a plasma parameter $\Lambda = \beta e^2 / \lambda_D \leq 1$ and the ratio of the cyclotron to the plasma frequency $\omega_c / \omega_p \geq 1$, where λ_D is the Debye screening length. Therefore, the thermal and particle transport across a steady magnetic field \vec{B} are expected to be driven by hydrodynamic modes at long wavelengths and low frequencies⁴⁻⁷ (convective cells, for instance). The corresponding highly nonlinear dynamics is now rather well understood by making use of the two-dimensional Coulomb gas as a starting point, which provides a rationale for the B^{-1} (Bohm-like) dependence of the observed transverse diffusion coefficient $D_{\perp} \simeq ck_B T / eB$. D_{\perp} is completely explained in terms of the equilibrium structure factors, when one introduces the guiding-center approximation (GCA) for the motion of charged particles. The time dependence of binary electric-field correlations thus get drastically simpli-

fied. The main purpose of the present work is twofold:

Inclusion of the right amount of classical and kinetic contributions ($\sim B^{-2}$) to the particle transport, by retaining the free streaming of the charges along \vec{B} . This goal is essentially achieved by adapting a hybrid formalism proposed by Vahala⁶ a few years ago.

Introduction of the nonzero \hbar corrections in the hydrodynamic transport, through a detailed evaluation of the equilibrium properties for a multicomponent plasma where the bare Coulomb interaction is replaced by the effective one which takes into account the diffraction (Heisenberg) and the symmetry (Pauli) effects. The basic formalism remains classical in any case. Actually, these small, albeit significant, corrections are expected to improve both the hydrodynamic and the kinetic contributions to D_{\perp} . In this respect, we feel that the theory developed here bears a particular concern to laser-driven plasma, where huge magnetic fields are likely to be produced near hot spots where nonlinear density and temperature gradients may develop megagauss-sized $\vec{\nabla} n \times \vec{\nabla} T$ magnetic fields \vec{B} during a time interval of several tens of picoseconds.

From the practical theoretic point of view, the most important transport coefficient, in relation with the above-mentioned huge B values, is the thermal conductivity, across the magnetic lines of force, which is expected to control a deleterious outward heat flow. The thermal conductivity is known to be a many-body problem which is far more involved than the particle diffusion coefficient D_{\perp} it-

self. We may conjecture, however, that in a large-field limit $\rho_L < \lambda_D$, or equivalently, $\Omega_i > \omega_{pi}$, the two lie on an almost equivalent footing. Moreover, in a case where $\Omega_i < \omega_{pi}$, D_\perp appears as an upper limit to the thermal conductivity. In fact, a few available pieces of numerical and experimental data tend to support a heat flow intermediate between a Bohm-like and a classical regime. We may thereby expect to be capable of drawing useful information from this more accessible quantity D_\perp . For a CO₂ laser with a wavelength of 10.6 μm , the critical density is roughly of the order of $10^{19}/\text{cm}^3$. The latter domain could become important in relation with recent speculations about the possibility that a self-generated intense magnetic field may penetrate, frozen, into the denser region because of a high conductivity prevailing there.³

Section II is essentially a review of the hydrodynamic formalism, discussed in detail by Montgomery *et al.*^{4,5} and by Vahala,⁶ of the diffusion coefficient D_\perp for the three-dimensional (3D) guiding-center plasma. Upon evaluating the autocorrelation function between the transverse components of fluctuating electric fields, the electron-electron, electron-ion, and ion-ion structure factors intervene automatically, accounting for the above-mentioned two quantum effects. They are derived in Sec. III and are used subsequently in Sec. IV in order to evaluate the quantum-corrected diffusion coefficient. The last section is devoted to concluding remarks.

II. SURVEY OF THE HYDRODYNAMIC FORMALISM

The Green-Kubo formalism for the linear response theory provides the particle diffusion coefficient D_\perp across an external magnetic field \vec{B} as

$$D_\perp = \frac{c^2}{B^2} \int_0^\infty d\tau \langle \vec{E}(\tau) \cdot \vec{E}(0) \rangle \quad (1)$$

in terms of an equilibrium canonical average of the two-point autocorrelation function for fluctuating electric fields. Since detailed calculations of D_\perp for both the three-dimensional⁴⁻⁶ (3D) and the extended ν -dimensional⁷ guiding-center (GC) plasma models have already been thoroughly studied, we here content ourselves to survey the underlying hydrodynamic formalism as concisely as possible. Let $\vec{x}(\tau)$ be the position of a test ion at time τ . Ignoring the spatial correlation between the test ion and the background plasma particles, we find D_\perp , in terms of the Fourier components of $\vec{E}[\vec{x}(\tau), \tau]$, as

$$D_\perp = \frac{c^2}{B^2} \sum_{\vec{k}} \int_0^\infty d\tau \langle \vec{E}_{\perp, \vec{k}}(\tau) \cdot \vec{E}_{\perp, -\vec{k}}(0) \rangle \langle e^{i\vec{k} \cdot \vec{x}(\tau)} \rangle \quad (2)$$

Eq. (2) implies the essence of the GC approximation, in that the two statistical averages in Eq. (2) can be expressed in terms of the two-time electric field correlations, such that

$$\langle \vec{E}_{\perp, \vec{k}}(\tau) \cdot \vec{E}_{\perp, -\vec{k}}(0) \rangle = \sum_{i,j} \frac{(4\pi)^2 e_i e_j}{V^2} \frac{k_\perp^2}{k^4} \langle e^{-i\vec{k} \cdot [\vec{x}_i(\tau) - \vec{x}_j(0)]} \rangle \quad (3)$$

and

$$\langle e^{i\vec{k} \cdot \vec{x}(\tau)} \rangle_{k_\parallel=0} = \exp \left[-\frac{c^2 k^2}{4B^2} \int_0^\tau d\tau' \int_0^\tau d\tau'' \langle \vec{E}_{\perp, \vec{k}}(\tau') \cdot \vec{E}_{\perp, -\vec{k}}(\tau'') \rangle \right], \quad (4)$$

where $\sum_{i,j}$ indicates the sum over all particles of the species i and j and V is the volume of a system. \vec{k} , \vec{k}_\perp , and \vec{k}_\parallel are the wave vector, its component perpendicular, and its component parallel to \vec{B} , respectively. In the 3D case, the GC approach is tantamount to describing the spatial diffusion of the test ion through small increments of $\vec{x}(\tau)$ and the velocity-space diffusion along \vec{B} via the equations of motion

$$\frac{d\vec{x}_\perp}{dt} = c^2 \frac{\vec{E}_\perp(t) \times \vec{B}}{B^2}, \quad \frac{d\vec{v}_\parallel}{dt} = \frac{e_i}{m_i} \vec{E}_\parallel(t). \quad (5)$$

The first of these two describes the $\vec{E} \times \vec{B}$ GC drift which is a good approximation in the limit of a zero Larmor radius, i.e., $(\Omega_i/\omega_{pi})^2 \gg 1$. Note that the initial position $\vec{x}(0)$ of the test ion may be set equal to zero and that its initial velocity obeys the Maxwell-Boltzmann distribution. We also remark that, upon evaluating $\exp[i\vec{k} \cdot \vec{x}(\tau)]$ with the aid of the cumulant expansion,⁶ an approximation is required to render tractable an expression with $\vec{k}_\parallel=0$. When turning our attention to the low-frequency and long-wavelength parts of the electric field spectra,⁶ it is expected that a free streaming of the particles along \vec{B} acts to destroy the electric field correlation between two-time points. If we ignore \vec{E}_\parallel , we then obtain

$$\langle \exp[i \vec{k} \cdot \vec{x}(\tau)] \rangle = \exp(-\frac{1}{2} k_{\parallel}^2 V_i^2 \tau^2), \quad \vec{k}_{\parallel} \neq 0 \quad (6)$$

where $V_i [(=k_B T/m_i)^{1/2}]$ is the ion thermal velocity. Performing now the summation over i and j in Eq. (3), we have

$$\langle \vec{E}_1(t) \cdot \vec{E}_1(0) \rangle = \frac{(4\pi)^2 n e^2}{V} \left[\sum_{k_{\parallel} \neq 0} \frac{k_{\perp}^2}{k^4} H_1(k) e^{-k_{\parallel}^2 V_i^2 t^2 / 2} + \sum_{k_{\parallel} = 0} \frac{1}{k_{\perp}^2} H_2(k_{\perp}) \exp \left[-\frac{k_{\perp}^2 c^2}{4B^2} \int_0^t dt' \int_0^{t'} dt'' \langle \vec{E}_1(t') \cdot \vec{E}_1(t'') \rangle \right] \right], \quad (7)$$

where $n (=n_i + n_e)$ is the total number density. The electron-electron, electron-ion, and ion-ion correlations come into play through two functions $H_1(\vec{k})$ and $H_2(\vec{k})$,⁸ both expressible in terms of the corresponding structure factors $S_{ee}(\vec{k})$, $S_{ei}(\vec{k})$, and $S_{ii}(\vec{k})$

$$H_1(\vec{k}) = \frac{Z^2}{(1+Z)^2} \left[e^{-k_{\parallel}^2 V_e^2 t^2 / 2} \left[1 + \frac{1}{Z} - n S_{ee}(\vec{k}) + n S_{ei}(\vec{k}) \right] + e^{-k_{\parallel}^2 V_i^2 t^2 / 2} [1 + Z - n S_{ii}(\vec{k}) + n S_{ei}(\vec{k})] \right], \quad (8a)$$

and

$$H_2(k_{\perp}) = Z + \frac{Z^2}{(1+Z)^2} n (-S_{ee} - S_{ii} + 2S_{ei}), \quad (8b)$$

where Z is the atomic number. S_{ij} 's which appear in the above expressions are defined, as usual, in terms of the pair correlation function $g_{ij}(r)$ through the self-explanatory relation

$$\langle e^{i \vec{k} \cdot [\vec{x}_i(\tau) - \vec{x}_j(0)]} \rangle = \delta_{\vec{k}, 0} - \frac{1}{V} \int d\vec{x} g_{ij}(x) e^{i \vec{k} \cdot \vec{x}} \equiv \delta_{\vec{k}, 0} - \frac{1}{V} S_{ij}(k), \quad i \neq j. \quad (9)$$

The two quantum effects mentioned in the Introduction are incorporated just in three S_{ij} 's which we shall specify in the next section. D_{\perp} is then calculated by virtue of the mean dispersion of the position of the test ion⁴⁻⁶ which reads as

$$R_{\perp}(t) = \frac{c^2}{4B^2} \int_0^t dt' \int_0^{t'} dt'' \langle \vec{E}_1(t'' - t') \cdot \vec{E}_1(0) \rangle \quad (10)$$

with $\dot{R}_{\perp}(\infty) = D_{\perp}/2$. Differentiating Eq. (10) twice with respect to t and using Eq. (7), we obtain the ordinary differential equation

$$\ddot{R}_{\perp}(t) = \epsilon_b \sum_{k_{\parallel} = 0} \frac{k_{\perp}^2}{2k_{\perp}^2} H_2(k_{\perp}) e^{-2k_{\perp}^2 R_{\perp}(t)} + \epsilon_b \sum_{\vec{k}, k_{\parallel} \neq 0} \frac{k_{\perp}^2 k_{\parallel}^2}{2k^4} H_1(k, t) e^{-k_{\parallel}^2 V_i^2 t^2 / 2 - k_{\parallel} D_{\parallel} t^3} \quad (11)$$

where $\epsilon_b = (4\pi)^2 e^2 n c^2 / B^2 V k_D^2$. Also, in Eq. (11),

the velocity-space diffusion coefficient D_{\parallel} is given by⁶

$$D_{\parallel} = \frac{e^2}{m_i^2} \int_0^{\infty} d\tau \langle E_{\parallel}(\tau) E_{\parallel}(0) \rangle \equiv \frac{1}{8\pi^{3/2}} \omega_{pi}^3 \lambda_D^2 \Lambda \ln \frac{1}{\Lambda}, \quad (12)$$

where $\Lambda = 1/(n\lambda_D^3) = 4\pi Z e^2 / k_B T \lambda_D$ with $\lambda_D^2 = k_B T / (4\pi n Z e^2)$. In the limit of a large volume, the discrete sum over k can be transformed into the integral through the identities

$$\sum_{k_{\parallel} = 0} \rightarrow \frac{V^{2/3}}{(2\pi)^2} \int d\vec{k}_{\perp} \quad (13)$$

and

$$\sum_{k_{\parallel} \neq 0} \rightarrow \frac{V}{(2\pi)^3} \int d\vec{k}.$$

In view of the subsequent analysis of Eq. (11), we find it convenient to introduce dimensionless variables by the transformations

$$z = 8\pi^2 \left[\frac{\Omega_i}{\omega_{pi}} \right]^2 \frac{P^{1/2} R_{\perp}}{\Lambda \lambda_D^2} \quad \text{and} \quad \tau = P^{1/2} \omega_{pi} t, \quad (14)$$

where $P = (2\pi\lambda_D/L)^2$ and $L (=V^{1/3})$ is an average size of the GC plasma. The volume-dependent parameter P , as we shall see below, plays a crucial role upon evaluating D_{\perp} . ω_{pi} and Ω_i are the ion plasma and the ion cyclotron frequencies, respectively. Replacing the discrete sum by the integral then gives the desired nondimensional equation

$$\frac{d^2z}{d\tau^2} = \frac{(1+Z)^2}{2Z^2} \left[\int_P^{1 \text{ or } Q} \frac{dx}{x} H_2(x) e^{-axz} + \frac{1}{2P^{1/2}} \int_P^Q \frac{dy}{\sqrt{y}} \int_P^Q dx \frac{x}{(x+y)^2} H_1(x,y,\tau) e^{-[(Z+1)/2Z + b\tau]\tau^2 y/P} \right], \quad (15)$$

where

$$Q = \left[\frac{8\pi}{\Lambda} \right]^2, \quad a = \frac{1}{4\pi^2} \left[\frac{\omega_{pi}}{\Omega_i} \right]^2 \frac{\Lambda}{P^{1/2}},$$

$$b = \frac{\Lambda \ln \left[\frac{1}{\Lambda} \right]}{8\pi^{3/2} P^{1/2}}, \quad (16)$$

$$x = (k_{\perp} \lambda_D)^2, \quad y = (k_{\parallel} \lambda_D)^2.$$

For typical values of the total density n , and an average size L , e.g., for the toroidal magnetized region of a laser-driven plasma spot, numerical values of B -independent parameters Λ , P , Q , and b as a function of T are given in Table I. Their order-of-magnitude estimate suggests to us an approximation to use in subsequent analyses. As for Eq. (15), two

remarks are in order: (1) Vahala's reasoning of splitting into two parts of the second integral in the right-hand side of Eq. (15), according to whether $y > [\Lambda \ln(1/\Lambda)]^2$ or not, that is, whether the free streaming along \vec{B} is dominant over the velocity-space diffusion or not, had the objective of emphasizing an important contribution from small but nonzero y values in the competition between these two processes. His rather forced argument can be remedied in quite a natural way by a purely mathematical requirement as will be discussed in Sec. IV. (2) The upper limit Q or 1 in the first integral indicates that the original k_{\perp} integration is cut either $k_{\perp, \max} = k_B T/e^2$ (kinetic limit) or at $k_{\perp, \max} = k_D$ (fluid limit). Finally, by multiplying both sides of Eq. (15) by $2 dz/d\tau$ and integrating once over τ from 0 to ∞ with the boundary conditions $z(0) = \dot{z}(0) = 0$ and $z(\infty) = \infty$, we obtain

$$[\dot{z}(\infty)]^2 = \frac{(1+Z)^2}{2Z^2} \left[\frac{2}{a} \int_P^{1 \text{ or } Q} \frac{dx}{x^2} H_2(x) + \frac{1}{P^{1/2}} \int_P^Q \frac{dy}{\sqrt{y}} \int_P^Q dx \frac{x}{(x+y)^2} \int_0^{\infty} d\tau \dot{z}(\tau) H_1(x,y,\tau) e^{-(g_2 + b\tau)\tau^2 y/P} \right], \quad (17)$$

with $g_2 = (1+Z)/2Z$. Setting

$$\beta = \frac{1}{a} \frac{(1+Z)^2}{Z^2} \int_P^{1 \text{ or } Q} \frac{dx}{x^2} H_2(x) \quad (18a)$$

and

$$f(y,\tau) = \frac{(1+Z)^2}{Z^2} \frac{1}{\sqrt{y}} \int_P^Q dx \frac{x}{(x+y)^2} H_1(x,y,\tau) \quad (18b)$$

we can write Eq. (17) formally as

$$[\dot{z}(\infty)]^2 = \beta + \frac{\dot{z}(\infty)}{2P^{1/2}} \int_P^Q dy \int_0^{\infty} d\tau f(y,\tau) e^{-(g_2 + b\tau)\tau^2 y/P}$$

$$- \frac{\dot{z}(\infty)}{2P^{1/2}} \int_P^Q dy \int_0^{\infty} d\tau \left[1 - \frac{\dot{z}(\tau)}{\dot{z}(\infty)} \right] f(y,\tau) e^{-(g_2 + b\tau)\tau^2 y/P}$$

$$\equiv \beta + (\alpha - \gamma) \dot{z}(\infty), \quad (19)$$

TABLE I. B -independent parameters Λ , Q , and b as a function of P [and of T through λ_D^2 , see the definition of P , below Eq. (14)]. Also, parameters $L = 10 \mu\text{m}$ and $n = 10^{21} \text{cm}^{-3}$. (n) denotes 10^n in Tables I to III.

P	1.0 (-5)	5.0 (-5)	1.0 (-4)	5.0 (-4)	1.0 (-3)	5.0 (-3)	1.0 (-2)
T	4.584(2)	2.292(3)	4.584(3)	2.292(4)	4.584(4)	2.292(5)	4.584(5)
Λ	7.844(-3)	7.016(-4)	2.481(-4)	2.219(-5)	7.844(-6)	7.016(-7)	2.481(-7)
Q	1.027(7)	1.283(9)	1.027(10)	1.283(12)	1.027(13)	1.283(15)	1.027(16)
b	2.700(-6)	1.618(-2)	4.623(-3)	2.387(-4)	6.546(-5)	3.156(-6)	8.469(-7)

where α and γ are the coefficients of $\dot{z}(\infty)$ in the second and the third terms of the right-hand side, respectively. The above derivation implies that, unless exact values of $\dot{z}(\infty)$ are known from a solution of Eq. (15), correct evaluation of γ is impossible. Referring to the exact numerical results that we shall discuss briefly in Sec. V, it is expected that neglecting γ compared to α gives an upper bound for $\dot{z}(\infty)$ and that the parameter dependence of the latter will not be seriously affected by this procedure. This is nothing else but Vahala's approximation. Thus, once $H_2(x)$ and $H_1(x, y, \tau)$ are known explicitly in terms of S_{ij} 's, we can evaluate α and β approximately and obtain D_{\perp} as

$$\frac{D_{\perp}}{\omega_{pi}\lambda_D^2} = \frac{1}{(2\pi)^2} \frac{\omega_{pi}^2}{\Omega_i^2} \Lambda \dot{z}(\infty) = aP^{1/2} \dot{z}(\infty). \quad (20)$$

III. QUANTUM-CORRECTED STRUCTURE FACTORS

For more than a decade, much effort⁹⁻¹¹ has been devoted to incorporating such quantum effects as the diffraction correction and the symmetry effect through a temperature-dependent interaction potential. These yield the quantum corrections to the equilibrium properties of the classical one-component plasma with a neutralizing background of opposite charge. For the three-dimensional two-component plasma it has been conjectured that the quantum treatment was required to secure the stability of a plus-minus pair. Though this leads to an appearance of bound states with negative discrete levels, a mean thermal energy high enough to break up most of bound states is responsible for a degree of ionization close to unity. The two-body stability will then be secured by the long-range Coulomb potential, interpolated with the $r \rightarrow 0$ limit of the wave function of the plus-minus pair, which is restricted to the interaction between ions and those electrons in the continuum. An additional quantum-mechanical requirement is that the Landau length $e^2/k_B T$ becomes comparable to or smaller than the electron thermal wavelength λ [$=\hbar/(2\pi m_e k_B T)^{1/2}$], which in turn should be smaller than λ_D . The importance of these effects, shown earlier by de Witt through an exact quantum many-body calculation,¹² may well be transcribed by replacing the classical Coulomb potential by the effective temperature-dependent pseudopotential^{8,13-15}

$$u_{ee}(r) = \frac{e^2}{r} (1 - e^{-r/\kappa}) + k_B T \ln 2 \exp \left[-\frac{1}{\pi \ln 2} \left(\frac{r}{\lambda} \right)^2 \right], \quad (21a)$$

$$u_{ei}(r) = -\frac{Ze^2}{r} (1 - e^{-\sqrt{2}r/\kappa}), \quad (21b)$$

$$u_{ii}(r) = \frac{Z^2 e^2}{r}. \quad (21c)$$

These expressions provide an excellent approximation to the effective potential in an intermediate- and high-temperature regime where the two quantum effects are safely decoupled from each other, so that the wave function of the interacting electron gas is given the symmetry of an ideal Fermi gas. A last quantum-mechanical requirement for an appearance of the discrete Landau levels to be neglected is that $\hbar\Omega_e \ll k_B T$, where Ω_e is the electron gyrofrequency. In a practical expression, this becomes

$$1.1577 \times 10^{-2} B \ll T,$$

where B is in units of MG and T in eV. The above inequality limits a region of the TB plane, when we calculate numerically such parameters as β_{cl} and β_{qu} as a function of T and B in Sec. IV.

Equations (21) show that quantum effects operate upon electrons as well as between electron and ion components. The first term in $u_{ee}(r)$ involves the factor $e^{-r/\kappa}$ which reflects the diffraction correction, while the second term stands for the symmetry property. In view of the definition of $S_{ij}(k)$'s as given by Eq. (9), they are related, in the limit of small Λ values, to the linearized pair correlation function $g_{ij}(r)$ through the relation

$$\begin{aligned} \frac{1}{V} \int d\vec{r} g_{ij}(r) e^{-i\vec{k}\cdot\vec{r}} &\cong \delta_{\vec{k},0} + \frac{1}{V} \int d\vec{r} v_{ij}(r) e^{-i\vec{k}\cdot\vec{r}} \\ &= \delta_{\vec{k},0} + \frac{1}{V} v_{ij}(k) \end{aligned}$$

Thus,

$$S_{ij}(k) = v_{ij}(k), \quad (22)$$

where $v_{ij}(k)$ is the Fourier-transformed resummed pseudopotential. In the case of a multicomponent plasma, consisting of n species of particles, the resummed potential is given as an infinite sum of chain graphs, in which a bond represents the bare potential $u_{ij}(r)$:

$$v_{ij}(r) = \text{---} \underset{i}{\circ} \text{---} \underset{j}{\circ} + \sum_{k=1}^n \text{---} \underset{i}{\circ} \text{---} \underset{k}{\circ} \text{---} \underset{j}{\circ} + \sum_{k,l=1}^n \text{---} \underset{i}{\circ} \text{---} \underset{k}{\circ} \text{---} \underset{l}{\circ} \text{---} \underset{j}{\circ} + \dots \quad (23)$$

The sum over i and j extends over every species. Fourier transforming Eq. (23) then yields

$$\vec{V}(k) = \vec{U}(k) \cdot [\vec{1} + \vec{U}(k) \cdot \vec{C}]^{-1}, \quad (24)$$

where $\vec{U}(k)$ and $\vec{V}(k)$ are the matrices composed of the Fourier-transformed bare and resummed pseudopotentials $u_{ij}(k)$ and $v_{ij}(k)$, respectively. $\vec{C} = nC_i \delta_{ij} / k_B T$ with $C_i (= N_i / \sum_j N_j)$ the relative concentration of the i th species. Other notations

are customary. When applied to a two-component plasma (i, j is the electron, one species of ion), we first obtain

$$u_{ee}(\kappa) = \frac{4\pi e^2 \lambda_D^2}{\kappa^2(1 + \eta^2 \kappa^2)} + ce^{-\alpha' \kappa^2}, \quad (25a)$$

$$u_{ei}(\kappa) = u_{ie}(\kappa) = -\frac{8\pi Z e^2 \lambda_D^2}{\kappa^2(2 + \eta^2 \kappa^2)}, \quad (25b)$$

$$u_{ii}(\kappa) = \frac{4\pi Z^2 e^2 \lambda_D^2}{\kappa^2}, \quad (25c)$$

where $\kappa = k \lambda_D$, $\eta = \hat{\lambda} / \lambda_D$, $\alpha' = (\pi \ln 2 / 4) \eta^2$, and $c = k_B T (\ln 2)^{5/2} (\pi \hat{\lambda})^3$. Substitution of Eqs. (25a)–(25c) into Eq. (24) then yields, after straightforward algebra, $\vec{V}(k)$, i.e., according to Eq. (12), $S_{ij}(k)$. The results are

$$nS_{ee}(\kappa) = n\beta V_{ee}(\kappa) = \frac{1}{Z} \left[\frac{1}{1 + \kappa^2 + \eta^2 \kappa^2 \left[\frac{Z}{1+Z} + \kappa^2 \right]} + \xi \left[1 - \frac{1}{(1+Z)(1+\kappa^2)} \right]^2 e^{-\alpha' \kappa^2} \right], \quad (26a)$$

$$nS_{ei}(\kappa) = -2 \left[\frac{1 + \eta^2 \kappa^2}{(2 + \eta^2 \kappa^2) \left[1 + \kappa^2 + \eta^2 \kappa^2 \left[\frac{Z}{1+Z} + \kappa^2 \right] \right]} - \frac{\xi}{2(1+Z)(1+\kappa^2)^2} \left[\frac{Z}{1+Z} + \kappa^2 \right] e^{-\alpha' \kappa^2} \right], \quad (26b)$$

$$nS_{ii}(\kappa) = Z \left[\frac{1 + \eta^2 \kappa^2}{1 + \kappa^2 + \eta^2 \kappa^2 \left[\frac{Z}{1+Z} + \kappa^2 \right]} + \frac{\xi}{(1+Z)^2(1+\kappa^2)^2} e^{-\alpha' \kappa^2} \right], \quad (26c)$$

where $\xi = Z \pi^3 (\ln 2)^{5/2} n \hat{\lambda}^3 = Z \pi^3 (\ln 2)^{5/2} \eta^3 \Lambda$. Redundant as it is, we repeat that the parameter η^2 reflects the diffraction correction, while the symmetry effect is characterized by ξ . Since, as was stated in the preceding section, we are concerned only with an order-of-magnitude estimate of these two effects, it is reasonable to assume $\eta^2, \xi \ll 1$ without worrying about which of the two is larger. We shall then retain terms up to the first order in η^2 and ξ in Eqs. (26a)–(26c). This procedure then demands that we should set $\alpha' = 0$, since, otherwise, we are led to take into account those terms of the order $\xi \eta^2$ and higher, which contradicts the assumption. Bringing Eqs. (26) back into Eqs. (8) and linearizing the resulting expressions for $H_1(\kappa, \tau)$ and $H_2(\kappa)$, we then obtain

$$H_1(\kappa, \tau)_{cl} = \frac{Z}{1+Z} \frac{\kappa^2}{1+\kappa^2} (e^{-g_1 y \tau^2 / P} + Z e^{-g_2 y \tau^2 / P}), \quad (27a)$$

$$H_1(\kappa, \tau)_{qu} = \frac{Z^2}{(1+Z)^2} \left[e^{-g_1 y \tau^2 / P} \left[\frac{\eta^2 \kappa^2 [Z + (2+Z)\kappa^2]}{2Z(1+\kappa^2)^2} - \xi \frac{\kappa^2 [Z + (1+Z)\kappa^2]}{Z(1+Z)(1+\kappa^2)^2} \right] + e^{-g_2 y \tau^2 / P} \left[-\frac{\eta^2 \kappa^2 (1-\kappa^2)}{2(1+\kappa^2)^2} + \xi \frac{\kappa^2}{(1+Z)(1+\kappa^2)^2} \right] \right], \quad (27b)$$

$$H_2(\kappa)_{cl} = Z \frac{\kappa^2}{1+\kappa^2}, \quad (28a)$$

$$H_2(\kappa)_{qu} = \eta^2 \frac{Z}{1+Z} \frac{\kappa^2}{(1+\kappa^2)^2} + \xi \frac{Z \kappa^2}{(1+Z)^2(1+\kappa^2)^2}, \quad (28b)$$

where $\kappa^2 = x + y$ in $H_1(\kappa, \tau)$ and $\kappa^2 = x$ in $H_2(\kappa)$. Also,

$$g_1 = (m_i/m_e)g_2 = (m_i/m_e)(1+Z)/2Z.$$

Suffixes cl and qu denote classical and quantum, respectively.

IV. EVALUATION OF $\dot{z}(\infty)$

Now, using Eqs. (28) for $H_2(x)$ in Eq. (18a), we obtain

$$\beta = \frac{(1+Z)^2}{az^2} \beta_{Q,1}, \quad (29)$$

$$\begin{aligned} \beta_Q &= Z \ln \frac{Q(1+P)}{(1+Q)P} + \frac{Z}{1+Z} \left[\eta^2 \left[\frac{1}{1+P} - \frac{1}{1+Q} \right] + \frac{\xi}{1+Z} \left[\ln \frac{Q(1+P)}{(1+Q)P} - \frac{1}{1+P} + \frac{1}{1+Q} \right] \right] \\ &\cong Z \ln \frac{1}{P} + \frac{Z}{1+Z} \left[\eta^2 + \frac{\xi}{1+Z} \left[\ln \frac{1}{P} - 1 \right] \right], \quad 1/Q, P \ll 1 \end{aligned} \quad (30a)$$

$$\begin{aligned} \beta_1 &= Z \ln \frac{1+P}{2P} + \frac{Z}{1+Z} \left[\eta^2 \left[\frac{1}{1+P} - \frac{1}{2} \right] + \frac{\xi}{1+Z} \left[\ln \frac{1+P}{2P} + \frac{1}{2} - \frac{1}{1+Q} \right] \right] \\ &\cong Z \ln \frac{1}{2P} + \frac{Z}{1+Z} \left[\frac{\eta^2}{2} + \frac{\xi}{1+Z} \left[\ln \frac{1}{2P} - \frac{1}{2} \right] \right], \quad P \ll 1. \end{aligned} \quad (30b)$$

β_Q and β_1 , both B -independent, stand for the integral with the upper limit Q and 1, respectively. As is easily seen from the definition, β depends on B only through the factor $1/a$ which is quadratic in B . Next, the integration over x in Eq. (18b), readily carried out, yields

$$\begin{aligned} f(y, \tau) &= \frac{1+Z}{Z} y^{-1/2} \left\{ \left[-y \ln \frac{Q+y}{P+y} + (1+y) \ln \frac{1+Q+y}{1+P+y} \right] (e^{-g_1 \tau^2 y/P} + e^{-g_2 \tau^2 y/P}) \right. \\ &\quad + \left\{ \frac{\eta^2}{2(1+Z)} \left[-Zy \ln \frac{Q+y}{P+y} + (2+Z+Zy) \ln \frac{1+Q+y}{1+P+y} \right. \right. \\ &\quad \quad \left. \left. - 2(1+y) \left[\frac{1}{1+P+y} - \frac{1}{1+Q+y} \right] \right] \right. \\ &\quad \left. - \frac{\xi}{(1+Z)^2} \left[-Zy \ln \frac{Q+y}{P+y} + (1+Z+Zy) \ln \frac{1+Q+y}{1+P+y} \right. \right. \\ &\quad \quad \left. \left. - (1+y) \left[\frac{1}{1+P+y} - \frac{1}{1+Q+y} \right] \right] \right\} e^{-g_1 \tau^2 y/P} \\ &\quad + \left\{ \frac{\eta^2}{2(1+Z)} \left[y \ln \frac{Q+y}{P+y} + (1-y) \ln \frac{1+Q+y}{1+P+y} \right. \right. \\ &\quad \quad \left. \left. - 2(1+y) \left[\frac{1}{1+P+y} - \frac{1}{1+Q+y} \right] \right] \right. \\ &\quad \left. + \frac{Z\xi}{(1+Z)^2} \left[-y \ln \frac{Q+y}{P+y} + y \ln \frac{1+Q+y}{1+P+y} \right. \right. \\ &\quad \quad \left. \left. + (1+y) \left[\frac{1}{1+P+y} - \frac{1}{1+Q+y} \right] \right] \right\} e^{-g_2 \tau^2 y/P}. \end{aligned} \quad (31)$$

We then encounter the delicate problem of the τ integration associated with the term $\exp[-(g+b\tau)\tau^2 y/P]$

[see Eq. (17)], which presumably led Vehala to argue that there must be a time τ_0 at which two terms in the exponent will be comparable, where, in the present context, we have either $g = g_1 + g_2$ or $g = 2g_2$. This amounts to stating that, for $\tau < \tau_0$, the free streaming term related to $\exp(-g\tau^2 y/P)$ is more important than the velocity-space diffusion term $\exp(-b\tau^3 y/P)$ and vice versa. His ingenious approach can be remedied, as was already described in Sec. II, by a purely mathematical reasoning. Let us first observe that the same type of integral¹⁶ as ours, namely,

$$\int_0^\infty d\tau e^{-\mu\tau^4 - 2v\tau^2} = \frac{1}{4} \left(\frac{2v}{\mu} \right)^{1/2} e^{v^2/2\mu} K_{1/4}(v^2/2\mu), \quad \text{Re}\mu > 0 \quad (32)$$

can be put, by setting $2v = gu$ and $\mu = bu$, into the form

$$I_1 \equiv \int_0^\infty d\tau e^{-(g+b\tau^2)\tau^2 u} = \frac{1}{4} \left(\frac{g}{b} \right)^{1/2} e^{g^2 u/8b} K_{1/4}(g^2 u/8b), \quad u \equiv y/P \quad (33)$$

which can be expanded either in the power or in the asymptotic series

$$I_1 \cong \begin{cases} \frac{\sqrt{2\pi}}{4\Gamma(\frac{3}{4})} \left(\frac{g^2}{4bu} \right)^{1/4} \left[1 - \frac{\Gamma(\frac{3}{4})}{\Gamma(\frac{1}{4})} \left(\frac{g^2 u}{4b} \right)^{1/2} + \dots \right], & \frac{g^2 u}{8b} < 1 \end{cases} \quad (34a)$$

$$I_1 \cong \begin{cases} \frac{1}{4} \left(\frac{2\pi}{u} \right)^{1/2} \left[1 - \frac{3}{16} \frac{4b}{g^2 u} + \dots \right], & \frac{g^2 u}{8b} > 1. \end{cases} \quad (34b)$$

These expressions are easily recovered either by first expanding $\exp(-bu\tau^4)$ in the Taylor series and then integrating over τ , a procedure which allows us to reach Eq. (34a), or by first expanding $\exp(-gu\tau^2)$ and then integrating, a procedure which leads to Eq. (34b). Going back to our integral, let us expand first either $\exp(-bu\tau^3)$ or $\exp(-gu\tau^2)$ and then integrate over τ . We obtain different expressions for the same I_2 as

$$I_2 = \int_0^\infty d\tau e^{-(g+b\tau)\tau^2 u} \cong \begin{cases} \frac{1}{2(2gu)^{1/2}} \sum_{n=0}^\infty \frac{(-)^n}{n!} \Gamma\left(\frac{3n+1}{2}\right) \frac{b^n}{(g^3 u)^{n/2}}, & \frac{b^2}{g^3 u} \leq 1 \end{cases} \quad (35a)$$

$$I_2 = \int_0^\infty d\tau e^{-(g+b\tau)\tau^2 u} \cong \begin{cases} \frac{1}{3(bu)^{1/3}} \sum_{n=0}^{n_{\max}} \frac{(-)^n}{n!} \Gamma\left(\frac{2n+1}{3}\right) \frac{(g^3 u)^{n/3}}{b^{2n/3}}, & \frac{b^2}{g^3 u} \geq 1. \end{cases} \quad (35b)$$

With these preparatory observations in mind, we can evaluate the τ integral in the second term of the right-hand side of Eq. (19), using Eq. (30). Retaining only two terms in the expansions given by Eqs. (35), we have

$$\begin{aligned} & \frac{Z^2}{(1+Z)^2} \int_P^Q dy \int_0^\infty d\tau f(y, \tau) e^{-(g_2+b\tau)y\tau^2/P} = \int_P^Q dy y^{-1/2} \int_0^\infty d\tau e^{-(g_2+b\tau)y\tau^2/P} \int_P^Q dx \frac{x}{(x+y)^2} H_1(x, y, \tau) \\ & \cong \frac{\sqrt{\pi}}{2} \left(\frac{P}{g} \right)^{1/2} \int_P^Q dy y^{-1/2} h_1(y) \left[1 - \frac{1}{\sqrt{\pi}} \left(\frac{P}{y} \right)^{1/2} \right] \\ & \quad + \frac{1}{3} \Gamma\left(\frac{1}{3}\right) \left(\frac{P}{b} \right)^{1/3} \int_P^R \frac{dy}{y^{1/3}} h_2(y) \left[1 - \frac{1}{\Gamma(\frac{1}{3})} \left(\frac{y}{R} \right)^{1/3} \right] \\ & \quad \quad \quad + \frac{\sqrt{\pi}}{2} \left(\frac{P}{2g_2} \right)^{1/2} \int_R^Q \frac{dy}{y^{1/2}} h_2(y) \left[1 - \frac{1}{\sqrt{\pi}} \left(\frac{R}{y} \right)^{1/2} \right], \quad R > P \\ & \quad \quad \quad + \frac{\sqrt{\pi}}{2} \left(\frac{P}{2g_2} \right)^{1/2} \int_P^Q \frac{dy}{y^{1/2}} h_2(y) \left[1 - \frac{1}{\sqrt{\pi}} \left(\frac{P}{y} \right)^{1/2} \right], \quad R < P \end{aligned} \quad (36)$$

where $R = b^2 P / (2g_2)^3$ and $g = g_1 + g_2 \cong (m_i/m_e)g_2$. Two functions $h_1(y)$ and $h_2(y)$ are obviously defined as

the coefficient of $\exp(-g_1\tau^2y/P)$ and $\exp(-g_2\tau^2y/P)$ in Eq. (31), respectively. The first line of Eq. (36) gives the coefficient of $\exp(-g_1\tau^2y/P)$ and $\exp(-g_2\tau^2y/P)$ in Eq. (31), respectively. The first line of Eq. (36) gives the contribution to α coming from the free streaming of electrons along \vec{B} , while the remaining part is related to the ion contribution. In a classical version, the former may be neglected with respect to the second or the third term, by noting that the free streaming of electrons tends to rapidly destroy the electric field correlations in this direction, because of the factor $g^{-1/2} \cong (m_e/m_i)^{1/2}$. Here we have to retain this term, in that, so small as it is, it could not be ignored with respect to quantum-corrected terms. Remaining elementary y integrations easily carried out, we finally obtain

$$\alpha \cong \frac{1}{4} \sqrt{\pi Z(1+Z)} \left[C + \frac{1}{Z} \left(\frac{2m_e}{m_i} \right)^{1/2} D \right] \quad (37)$$

where

$$D = \frac{1}{2} (\ln Q)^2 + \ln Q \ln \frac{1}{P} - \frac{\pi^2}{12} + \frac{\eta^2}{2(1+Z)} \left[(2+Z) \left[\frac{1}{2} (\ln Q)^2 + \ln Q \ln \frac{1}{P} - \frac{\pi^2}{12} \right] - 2 \ln \frac{Q}{2P} \right] - \frac{\xi}{(1+Z)^2} \left[(1+Z) \left[\frac{1}{2} (\ln Q)^2 + \ln Q \ln \frac{1}{P} - \frac{\pi^2}{12} \right] - \ln \frac{Q}{2P} \right] \quad (38)$$

$$C = \frac{1}{2} (\ln Q)^2 + \ln Q \ln \frac{1}{R} - \frac{2}{\sqrt{\pi}} \ln Q + \frac{4}{\sqrt{\pi}} \Gamma\left(\frac{1}{3}\right) \left[1 - \left(\frac{P}{R} \right)^{1/6} \right] \ln Q - \frac{\pi^2}{12} + 4\sqrt{\pi} R^{1/2} + \frac{\eta^2}{2(1+Z)} \left[\frac{1}{2} (\ln Q)^2 + \ln Q \ln \frac{1}{R} - 2 \ln \frac{Q}{2R} - \frac{\pi^2}{12} \right] + \frac{\xi}{(1+Z)^2} \ln \frac{Q}{2R}, \quad R > P \quad (39a)$$

$$= \frac{1}{2} (\ln Q)^2 + \ln Q \ln \frac{1}{P} - \frac{2}{\sqrt{\pi}} \ln Q - \frac{\pi^2}{12} + 4\sqrt{\pi} P^{1/2} + \frac{\eta^2}{2(1+Z)} \left[\frac{1}{2} (\ln Q)^2 + \ln Q \ln \frac{1}{P} - 2 \ln \frac{Q}{2P} - \frac{\pi^2}{12} \right] + \frac{\xi}{(1+Z)^2} \ln \frac{Q}{2P}, \quad R < P. \quad (39b)$$

Equations (37) and (38) are accurate up to the order $P^{1/2}$ and/or $R^{1/2}$ which is smaller than unity and such higher-order terms as $1/Q$, P , $P \ln P$, etc., have been systematically neglected. This follows directly from the definition of R , i.e.,

$$R = \frac{b^2 P}{(2g_2)^3} = \frac{Z^3}{64\pi^3(1+Z)^3} \left[\Lambda \ln \frac{1}{\Lambda} \right]^2 \leq \frac{1}{64\pi^3 e^2} = 6.82 \times 10^{-5},$$

when

$$\Lambda < 1$$

and that of P , i.e., $P = (2\pi\lambda_D/L)^2$. Notice that α , thus calculated, depends on three B -independent parameters Q , P , and/or R . Therefore, $\dot{z}(\infty)$, as given by the formal solution of Eq. (19), namely,

$$\dot{z}(\infty) = \frac{1}{2} [\alpha + (\alpha^2 + 4\beta)^{1/2}] \quad (40)$$

depends on B only through β . By inspection of Eq.

(18a) for β and Eq. (16) for a , β is proportional to $(\Omega_i/\omega_{pi})^2$, that is, to B^2 . This implies that, whenever $4\beta \gg \alpha^2$, $\dot{z}(\infty) \sim \sqrt{\beta}$ and that, in the opposite limit, $\dot{z}(\infty) \sim \alpha$. Correspondingly, D_{\perp} is proportional to $1/B$ (Bohm-type) in the former case and turns out to be of the classical type in the latter. Between the two, i.e., when $\alpha^2 \sim 4\beta$, a hybrid diffusion takes place. In order to examine quantitatively these situations, extensive numerical analysis has been carried out. For fixed values of L (characteristic plasma size) and n (total number density), we have varied P , which amounts to varying T (temperature). In Table II, numerical values of η^2 , η/Λ , α_{cl} (classical part of α), and α_{qu} (quantum part of α) as a function of P are tabulated. Since we are interested in the parameter range where $\Lambda \ll 1$, we first recognize that the inequality $\alpha_{qu} \ll \alpha_{cl}$ always holds. In Table III, such B -dependent quantities as a , β_{cl} (classical part of β), and β_{qu} (quantum part of β) are also shown as a function of P (horizontal) and of B (vertical). On the left margin of this table the upper number indicates Ω_i/ω_{pi} and the lower one

TABLE II. B -independent parameters η^2 , η/Λ , α_{cl} , and α_{qu} as a function of P . η^2 measures the diffraction correction and η/Λ the ratio of the symmetry effect to the diffraction one. For the definition of η and α , see the definitions below Eqs. (25) and (19). Also, parameters $L = 10 \mu\text{m}$ and $n = 10^{21} \text{cm}^{-3}$.

P	1.0 (-5)	5.0 (-5)	1.0 (-4)	5.0 (-4)	1.0 (-3)	5.0 (-3)	1.0 (-2)
T	4.584 (2)	2.292 (3)	4.584 (3)	2.292 (4)	4.584 (4)	2.292 (5)	4.584 (5)
η^2	1.045(-6)	4.178(-8)	1.045(-8)	4.178(-10)	1.045(-10)	4.178(-12)	1.045(-12)
η/Λ	1.303(-1)	2.913(-1)	4.120(-1)	9.213 (-1)	1.303 (0)	2.913 (0)	4.120 (0)
α_{cl}	2.023(2)	2.737(2)	3.601(2)	3.847 (2)	4.203 (2)	5.060 (2)	5.446 (2)
α_{qu}	4.959(-5)	2.844(-6)	8.137(-7)	4.304 (-8)	1.196 (-8)	5.825(-10)	1.527(-10)

the corresponding B values in gauss. We should remark that there exists a domain where β_{qu} becomes comparable to or larger than α_{cl} . In view of checking this rather surprising result, the ratio of β_{qu}/α_{cl} is calculated by virtue of Eqs. (37)–(39), (29), and (30a). It is given by

$$\frac{\beta_{qu}}{\alpha_{cl}} = 16 \left(\frac{\pi}{2} \right)^{1/2} \left(\frac{\Omega_i}{\omega_{pi}} \right)^2 \frac{a_0}{L} \times \frac{1 + 0.139 \left[\frac{k_B T}{\epsilon_0} \right]^{1/2} \left[\ln \frac{1}{P} - 1 \right]}{\ln Q \left[\ln Q + 2 \ln \frac{1}{P} \right]}, \quad (41)$$

where $a_0 (= \hbar^2/m_e e^2 = 5.29 \times 10^{-5} \mu\text{m})$ is the Bohr radius and $\epsilon_0 (= m_e e^4/2\hbar^2 = 1 \text{ Ry})$ the ionization energy of the hydrogen atom. Even if Q and $1/P$ are much larger than unity, their logarithms are at most of the order of several tens. Since a_0/L is a very small number (of the order of 10^{-5}), the inequality $\beta_{qu}/\alpha_{cl} \geq 1$ may hold only if $(\Omega_i/\omega_{pi})^2 \gg 1$ and $k_B T/\epsilon_0 \gg 1$, that is, for extremely high temperatures and very intense magnetic fields. On the other hand, zigzag lines in the table divide the parameter space spanned by B and T into two regions; at their right side, degenerate Landau levels need not be considered as a first approximation. These lines are traced according to the inequality already discussed in Sec. III, namely, $0.0116B \text{ (MG)} \ll T \text{ (eV)}$.

In view of visualizing all these features, several figures are also presented. In Fig. 1, α is plotted as a function of T_e for different sets of parameters n and L . In Fig. 2, the variation of β vs P (abscissa) and Ω_i/ω_{pi} (ordinate) is illustrated, where β is the sum of β_{cl} and β_{qu} . Note that in Figs. 2–4, the two axes are scaled by the natural logarithms. Values of β are normalized to unity by its value at $P = 10^{-3}$ and $\Omega_i/\omega_{pi} = 10^4$. We see that, since P is proportional to T through λ_D^2 , β increases rapidly in the domain of high temperatures and strong magnetic

fields. When we turn our attention to β_{qu} , we recognize in Fig. 3 that, though always smaller than its classical part β_{cl} (see Table III), it may compete with, or become even larger than, the classical part of α , simply due to a rapid decrease, with increasing B , of the factor a , which is inversely proportional to B^2 . In Fig. 4, we show the variation of D_1 vs P and Ω_i/ω_{pi} . Its values are normalized to unity as for β . It is observed that D_1 behaves like β . Finally, in Fig. 5, D_1 is plotted as a function of Ω_i/ω_{pi} for fixed values of n and L . The Bohm regime is easily distinguished from the classical regime.

V. CONCLUDING REMARKS

The validity of discussions, given at the end of Sec. II, concerning the complete neglect of γ with respect to α in Eq. (19) should now be carefully examined with recourse to a numerical evaluation of γ , which requires the knowledge of $\dot{z}(\tau)$ as a function of τ . To this end, the nonlinear differential equation (15) was solved by means of the Runge-Kutta method on the one hand and of the Milne method with variable steps on the other hand. In order to start iteration, we first need the values of $z(\tau)$ and $\dot{z}(\tau)$ for small values of τ , since the initial conditions $z(0) = \dot{z}(0) = 0$ are of no use for the numerical solution of Eq. (15). The meaning of “small τ values” will be clarified in the subsequent discussion. Since the first integral on the right-hand side of Eq. (15) is straightforward, it is reasonable to set $\tau = 0$ for the second integral involving $H_1(x, y, \tau)$. Restricting ourselves to the classical limit, in which case all quantum terms are neglected, an approximation that is valid for almost all of the parameter space spanned by n , T , and B , we first obtain

$$\ddot{z}(\tau) \cong 2e^{az} [E_1(az) - E_1(a\tau Q)] + \left[\frac{Q}{P} \right]^{1/2} (2 \ln 2 + 1 + \pi), \quad (42)$$

TABLE III. B -dependent parameters a , β_{cl} , β_{qu} , $\dot{z}(\infty)$, and $D_1/\omega_{pl}\lambda_D^2$ as a function of P . For the definition of a , β , $\dot{z}(\infty)$, and D_1 , see Eqs. (16), (18a), and (20), respectively. Also, parameters $L = 10 \mu\text{m}$ and $n = 10^{21} \text{cm}^{-3}$.

P	1.0 (-5)	5.0 (-5)	1.0 (-4)	5.0 (-4)	1.0 (-3)	5.0 (-3)	1.0 (-2)
1.0 (0)	6.283(-2)	2.513(-3)	6.283(-4)	2.513(-5)	6.283(-6)	2.513(-7)	6.283(-8)
3.073(9)	7.329(2)	1.576(4)	5.864(4)	1.210(6)	4.398(6)	8.441(7)	2.938(8)
	3.157(-4)	5.681(-4)	7.308(-4)	1.287(-3)	1.621(-3)	2.621(-3)	3.113(-3)
	2.058(2)	3.226(2)	4.395(2)	1.309(3)	2.318(3)	9.444(3)	1.742(4)
	4.089(-3)	5.733(-3)	2.761(-3)	7.356(-4)	4.605(-4)	1.678(-4)	1.094(-4)
1.0 (1)	6.283(-4)	2.513(-5)	6.283(-6)	2.513(-7)	6.283(-8)	2.513(-9)	6.283(-10)
3.073(10)	7.329(4)	1.576(6)	5.864(6)	1.210(8)	4.398(8)	8.441(9)	2.938(10)
	3.157(-2)	5.681(-2)	7.308(-2)	1.287(-1)	1.621(-1)	2.621(-1)	3.113(-1)
	3.901(2)	1.400(3)	2.579(3)	1.119(4)	2.118(4)	9.213(4)	1.717(5)
	7.752(-4)	2.488(-4)	1.621(-4)	6.290(-5)	4.209(-5)	1.637(-5)	1.079(-5)
1.0 (2)	6.283(-6)	2.513(-7)	6.283(-8)	2.513(-9)	6.283(-10)	2.513(-11)	6.283(-12)
3.073(11)	7.329(6)	1.576(8)	5.864(8)	1.210(10)	4.398(10)	8.441(11)	2.938(12)
	3.157(0)	5.681(0)	7.308(0)	1.287(1)	1.621(1)	2.621(1)	3.113(1)
	2.810(3)	1.269(4)	2.437(4)	1.102(5)	2.099(5)	9.190(5)	1.714(6)
	5.584(-5)	2.256(-5)	1.531(-5)	6.192(-6)	4.171(-6)	1.633(-6)	1.077(-6)
1.0 (3)	6.283(-8)	2.513(-9)	6.283(-10)	2.513(-11)	6.283(-12)	2.513(-13)	6.283(-14)
3.073(12)	7.329(8)	1.576(10)	5.864(10)	1.210(12)	4.398(12)	8.441(13)	2.938(14)
	3.157(2)	5.681(2)	7.308(2)	1.287(3)	1.621(3)	2.621(3)	3.113(3)
	2.717(4)	1.257(5)	2.423(5)	1.100(6)	2.097(6)	9.188(6)	1.714(7)
	5.399(-6)	2.234(-6)	1.522(-6)	6.182(-7)	4.167(-7)	1.633(-7)	1.077(-7)
1.0 (4)	6.283(-10)	2.513(-11)	6.283(-12)	2.513(-13)	6.283(-14)	2.513(-15)	6.283(-16)
3.073(14)	7.329(10)	1.576(12)	5.864(12)	1.210(14)	4.398(14)	8.441(15)	2.938(16)
	3.157(4)	5.681(4)	7.308(4)	1.287(5)	1.621(5)	2.621(5)	3.113(5)
	2.708(5)	1.256(6)	2.412(6)	1.100(7)	2.097(7)	9.187(7)	1.714(8)
	5.381(-7)	2.231(-7)	1.522(-7)	6.181(-8)	4.167(-8)	1.633(-7)	1.077(-8)

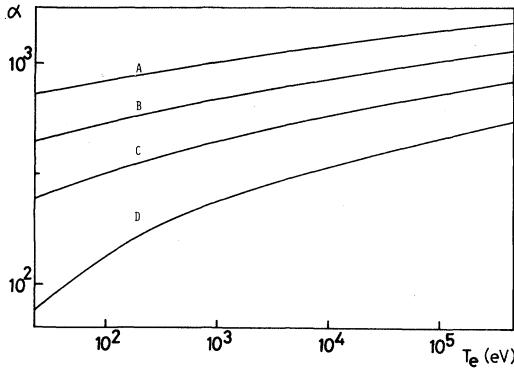


FIG. 1. α ($=\alpha_{cl}+\alpha_{qu}$) vs T_e for different set of parameters n and L . The curves correspond to the set: A, $n=10^{25}$ cm^{-3} , $L=50$ μm ; B, $n=10^{25}$ cm^{-3} , $L=10$ μm ; C, $n=10^{21}$ cm^{-3} , $L=50$ μm ; and D, $n=10^{21}$ cm^{-3} , $L=10$ μm .

where, to simplify the situation, we have set $Z=1$ and made use of the conditions $P, 1/Q \ll 1$. Next, we assume $azQ \ll 1$, which requires a small starting value of τ . The series expansion of the exponential integrals being then in order, Eq. (42) reads

$$[\dot{z}(\tau)]^2 = 2c_0z - c_2z^2 \tag{43}$$

with

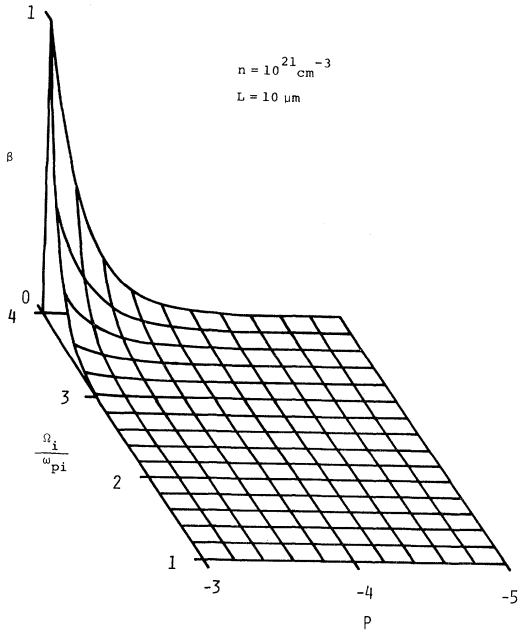


FIG. 2. Variation of β ($=\beta_{cl}+\beta_{qu}$) as a function of P (abscissa) and Ω_i/ω_{pi} (ordinate) for typical values of n and L pertinent to a laser-driven plasma. In Figs. 2–4, the two axes are scaled by the natural logarithm.

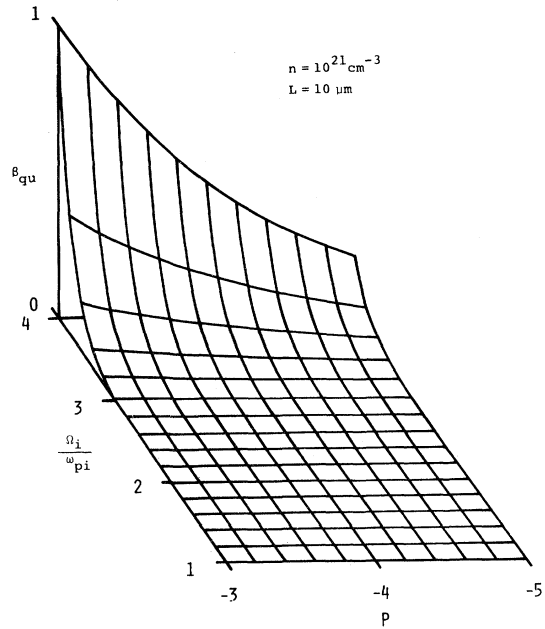


FIG. 3. Variation of β_{qu} as a function of P (abscissa) and of Ω_i/ω_{pi} (ordinate), with the same values of n and L as in Fig. 2.

$$c_0 = 2 \ln Q + (2 \ln 2 + 1 + \pi)(Q/P)^{1/2} \\ \cong (2 \ln 2 + 1 + \pi)(Q/P)^{1/2}$$

and

$$c_2 \cong 2aQ .$$

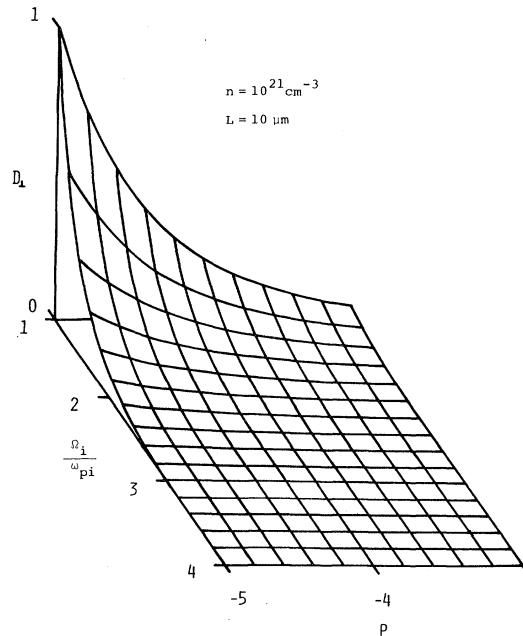


FIG. 4. Variation of D_1 vs P and Ω_i/ω_{pi} .

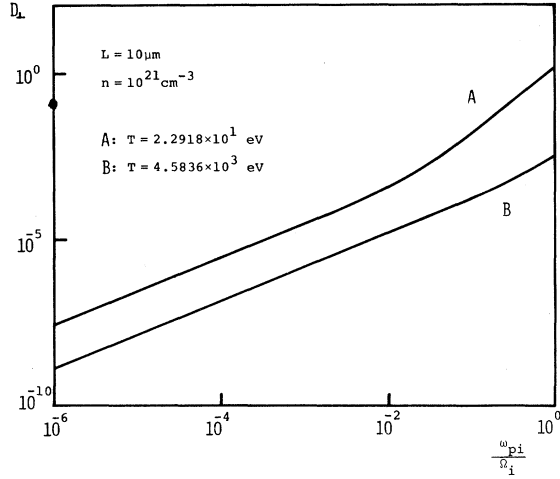


FIG. 5. D_{\perp} vs ω_{pi}/Ω_i , with the same values of n and L as in Fig. 2. Curve A is for $T=22.9$ eV and curve B for $T=4.58$ keV. Though the scaling unit of two axes is different, the Bohm regime is easily distinguished from the classical regime.

The solution to Eq. (43) is given by

$$z(\tau) \cong \frac{c_0}{c_2} \sin^2 \left[\frac{\sqrt{c_2}}{2} \tau \right]. \quad (44)$$

The validity of the condition $azQ \ll 1$ is *a posteriori* ensured by $\tau \ll 2/(c_0 c_2)^{1/2}$ or, more explicitly, by

$$\tau \ll 0.60150 \left[\frac{P}{a^2 Q^3} \right]^{1/4}. \quad (45)$$

The initial conditions for $z(\tau)$ and $\dot{z}(\tau)$ should be evaluated for any value of τ , say τ_i , which satisfies the above constraint. For the numerical solution of Eq. (15), iteration started at $\tau = \tau_i$, so that $aQz(\tau_i) < 10^{-4}$. Corresponding initial conditions $z(\tau_i)$ and $\dot{z}(\tau_i)$ are calculated, using Eq. (44). They are: $\tau_i = 1.0 \times 10^{-11}$, $z(\tau_i) = 2.0427 \times 10^{-17}$, and $\dot{z}(\tau_i) = 4.8045 \times 10^{-6}$. A typical set of data used are: $n = 10^{21} \text{ cm}^{-3}$, $T = 0.5 \text{ keV}$, $L = 10 \text{ } \mu\text{m}$, and $B = 10^6 \text{ G}$. Correspondingly, we have: $P = 5.4542 \times 10^{-6}$, $Q = 1.6657 \times 10^6$, and $a = 3.9898 \times 10^6$. These parameters inserted into Eqs. (30a), (37), and (40) yield $\alpha \approx 80.753$, $\beta \approx 6.0750 \times 10^{-6}$ and thus $\dot{z}(\infty) = 80.753$. The behavior of $\dot{z}(\tau)$ is illustrated in Fig. 6. The iteration scheme for the solution of Eq. (15) was checked, upon evaluating numerically the factor γ by virtue of the $\dot{z}(\tau)$ values sampled in the range $\tau_i < \tau < \tau_f$, such that, at τ_f , $\dot{z}(\tau)$ practically saturates. The resulting γ value is $\gamma = 40.13$, leading to

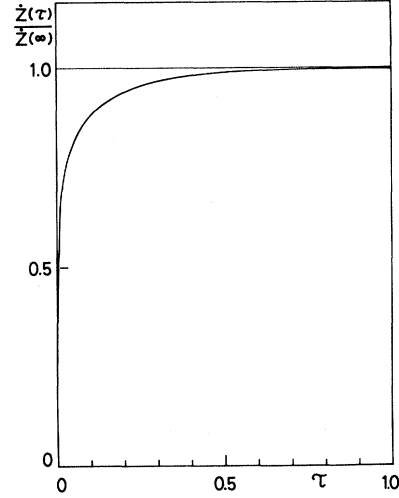


FIG. 6. Temporal variation of $\dot{z}(\tau)/\dot{z}(\infty)$ for a set of parameters $n = 10^{21} \text{ cm}^{-3}$, $T = 0.5 \text{ keV}$, $L = 10 \text{ } \mu\text{m}$, and $B = 10^6 \text{ G}$.

$\dot{z}(\infty)_{\text{numerical}} = 40.30$. The approximate analytical result is thus seen to be twice as large as the numerical value. This is why we have stated in Sec. II that Vahala's analysis, and thus ours, gives an upper bound to the exact value of $\dot{z}(\infty)$.

So far, we have discussed the diffraction and the symmetry effects on the diffusion coefficient D_{\perp} within the framework of the hydrodynamic GC model. With the aid of nondimensional parameters introduced in Sec. II and with inclusion of the quantum-corrected structure factors S_{ee} , S_{ei} , and S_{ii} evaluated in Sec. III, we have obtained explicit expressions for both the classical and the quantum parts of α and β , with which to find $\dot{z}(\infty)$ through Eq. (40) and D_{\perp} through Eq. (20). Our result gives an upper bound to the numerically evaluated "exact" D_{\perp} values. As was argued at the end of Sec. IV, inspection of Eq. (40) suggest that, whenever $\beta \gg \alpha^2$, $\dot{z}(\infty) \sim \sqrt{\beta}$ and that, in the opposite limit, $\dot{z}(\infty) \sim \alpha$. Correspondingly, D_{\perp} becomes proportional to $1/B$ (Bohm type) in the former case and is of the classical type ($\sim 1/B^2$) in the latter. Between the two, i.e., when $\beta \sim \alpha^2$, a hybrid diffusion takes place. Our main results and comments are enumerated as follows:

(1) The symmetry effect characterized by the parameter η^3/Λ is roughly η/Λ times the diffraction parameter η^2 . The importance of the former thus crucially depends on the ratio η/Λ (see Table II).

(2) As a result of extensive numerical analysis, in which n and L are fixed and T and B are widely varied, we have found that the quantum part of β ,

though always much smaller than its classical part, competes with, or may become even larger than, the classical part of α , for high T and extremely large B values (see Table III). This corresponds to the Bohm regime, where the position-space diffusion dominates the velocity-space diffusion. In other terms, the role of fluctuating electric fields \vec{E}_{\parallel} (along the magnetic lines of force) is not effective enough to cause an appreciable velocity-space diffusion, in spite of an extremely strong confining magnetic field. Increase of β_{qu} may be simply attributed, as is obvious from Eq. (18a), to a noticeable decrease, with increasing B , of the parameter α which is inversely proportional to B^2 .

(3) In connection with this rather surprising result, we notice that a favorable situation may also be realized in a strongly magnetized semiconductor even at room temperature, for which the quantum part of D_{\perp} would really compete with its classical part. Apparently, large B values extend the range of validity of the classical regime. This effect is

especially remarkable in the present GC model where ions are mostly confined transversally to the magnetic field, in agreement with recent computations¹⁷ on the two-dimensional melting transition in a strong magnetic field.

(4) The parameter β calculated in the text can be globally modified to include a finite gyroradius effect¹⁸ by multiplying it with the factor $[1 + (\omega_{pi}/\Omega_i)^2]^{-1}$. However, in the domain where $(\Omega_i/\omega_{pi})^2 \gg 1$, this factor reduces to unity and thus the above-mentioned effect hardly comes into play.

(5) Proper account of the degenerate Landau levels for the evaluation of a more elaborate quantum-corrected D_{\perp} is left open for a future work.

ACKNOWLEDGMENTS

Enlightening discussions we have had with Dr. H. Totsuji are gratefully acknowledged.

*Laboratoire associé au CNRS.

¹M. Ruderman, J. Phys. (Suppl.) C **2**, 125 (1980).

²G. Gerlich, H. Kagerman, and E. W. Richter, Physica **96C**, 347 (1979).

³C. E. Max, W. M. Manheimer, and J. J. Thomson, Phys. Fluids **21**, 128 (1978).

⁴D. Montgomery, C. S. Liu, and G. Vahala, Phys. Fluids **15**, 815 (1972).

⁵D. Montgomery, in *Les Houches Lecture Notes* (Gordon and Breach, New York, 1975).

⁶G. Vahala, Phys. Fluids **16**, 1876 (1973).

⁷C. Deutsch, Phys. Rev. A **17**, 909 (1978).

⁸C. Deutsch, Y. Furutani, and M. M. Gombert, Phys. Rep. **69**, 85 (1981).

⁹G. Kelbg, Ann. Phys. (Leipzig) **12**, 219 (1963).

¹⁰A. Barker, J. Chem. Phys. **55**, 1751 (1971).

¹¹B. Davis and R. G. Storer, Phys. Rev. **171**, 150 (1968).

¹²H. de Witt, J. Math. Phys. **7**, 616 (1966).

¹³C. Deutsch, M. M. Gombert, and H. Minoo, Phys. Lett. **66A**, 381 (1978).

¹⁴H. Minoo, M. M. Gombert, and C. Deutsch, Phys. Rev. A **23**, 924 (1981).

¹⁵M. M. Gombert, Thèses d'Etat, Orsay, 1981 (unpublished).

¹⁶I. S. Gradshteyn and I. M. Ryzhik, in *Table of Integrals, Series, and Products*, translation edited by A. Jeffrey (Academic, New York, 1965).

¹⁷H. Fukuyama and D. Yoshioka, J. Phys. Soc. Jpn. **48**, 1853 (1980).

¹⁸H. Okuda and J. M. Dawson, Phys. Fluids **16**, 408 (1973).